

Synthesis of Large Unequally Spaced Planar Arrays Utilizing Differential Evolution With New Encoding Mechanism and Cauchy Mutation

Foxiang Liu, Yanhui Liu^{ID}, *Senior Member, IEEE*, Feng Han^{ID}, *Member, IEEE*, Yong-Ling Ban^{ID}, and Y. Jay Guo^{ID}, *Fellow, IEEE*

Abstract—This article presents a differential evolution algorithm with a new encoding mechanism and Cauchy mutation (DE-NEM-CM) for optimizing large unequally spaced planar array layouts with the minimum element spacing constraint. In the new encoding mechanism, each individual represents a certain element position rather than an entire array layout used in traditional stochastic optimization algorithms. Such an encoding mechanism has the following advantages: 1) in each individual updating, the array pattern can be efficiently evaluated by only considering the radiation contribution variation from one element movement, which can greatly reduce the computational time; 2) it naturally facilitates the generated new array layout in population updating to meet the minimum element spacing constraint, and 3) each individual is searched always in 2-D space as the array size increases. These advantages enable it to be very suitable for synthesizing large arrays. Besides, DE serves as a search engine, and Cauchy mutation with chaotic mapping is proposed to enhance the local search while preserving the diversity of the population. A set of experiments for synthesizing different types of unequally spaced planar arrays in both narrow-and broadband applications are conducted. Synthesis results show that the proposed method achieves much lower sidelobe level than some state-of-the-art stochastic optimization methods for all the test cases. Importantly, the proposed method is much more efficient than conventional stochastic optimization algorithm especially for the case of synthesizing large unequally spaced planar array layouts. A array layout optimization with more than 1000 elements can be achieved within acceptable CPU time cost, which has not yet been reported for the existing stochastic optimization methods without resorting to supercomputing facilities.

Manuscript received October 8, 2019; accepted December 31, 2019. Date of publication February 3, 2020; date of current version June 2, 2020. This work was supported in part by the Natural Science Foundation of China (NSFC) under Grant 61871338, in part by the Science and Technology Research Project of Fujian Province under Grant 2017J0017, and in part by the University of Technology Sydney. (*Corresponding author: Yanhui Liu*)

Foxiang Liu and Feng Han are with the Institute of Electromagnetics and Acoustics, Xiamen University, Xiamen 361005, China, and also with the Fujian Provincial Key Laboratory of Electromagnetic Wave Science and Detection Technology, Xiamen University, Xiamen 361005, China.

Yanhui Liu is with the School of Electronic Science and Engineering, University of Electronic Science and Technology of China, Chengdu 611731, China, also with the Institute of Electromagnetics and Acoustics, Xiamen University, Xiamen 361005, China, and also with the Global Big Data Technologies Centre, University of Technology Sydney (UTS), Ultimo, NSW 2007, Australia (e-mail: yhliu@uestc.edu.cn).

Yong-Ling Ban is with the School of Electronic Science and Engineering, University of Electronic Science and Technology of China, Chengdu 611731, China.

Y. Jay Guo is with the Global Big Data Technologies Centre, University of Technology Sydney (UTS), Ultimo, NSW 2007, Australia.

Color versions of one or more of the figures in this article are available online at <http://ieeexplore.ieee.org>.

Digital Object Identifier 10.1109/TAP.2020.2969741

Index Terms—Cauchy mutation, differential evolution (DE), encoding mechanism, large planar arrays, unequally spaced arrays.

I. INTRODUCTION

UNEQUALLY spaced antenna arrays have been widely applied in radars, sonars, and wireless communication systems [1]–[3]. Compared with uniformly spaced arrays, they can exploit element positions as an additional degrees of freedom (DOF) to achieve better radiation characteristics such as low sidelobe and grating lobe levels (GLLs). Furthermore, by using optimized element positions, the unequally spaced array is capable of reducing the number of elements and the associated radio frequency (RF) components, which is significant for the application where the allowable weight, space, and cost of the radiation system may be strictly limited.

Over the last few decades, various unequally spaced array synthesis methods have been presented [4]–[18]. Usually, analytical methods such as those in [4]–[6] can produce a solution to element positions in a highly efficient manner, but they cannot control the obtained sidelobe distribution very well. In [7]–[9], some iterative convex optimization techniques are presented in which unequally spaced array synthesis problems are formulated as performing iterative weighted L_1 -norm optimization with multiple convex constraints. The sidelobe level can be accurately controlled by using multiple pattern constraints. However, one limitation with the iterative convex optimization techniques is that the minimum element spacing is hard to control and consequently the synthesized arrays are sometimes impractical. The matrix pencil methods in [10]–[12] and the compressive sensing techniques in [13]–[15] can also be applied to reconstruct element positions and excitations by matching the synthesized pattern to a reference one in both amplitude and phase distribution. However, prescribing a realizable reference field pattern is a challenge itself, and one may need to resort to some other synthesis techniques. If the reference pattern is chosen inappropriately, the synthesized result will not be satisfactory. Besides, some other sparse array techniques presented in [19]–[21] are also computationally efficient, but they are effective only for designing thinned arrays which are obtained by turning off part of elements from prescribed equally spaced arrays. Since the realized element spacings in the thinned array are integer multiples of a preset spacing, the feeding network structure is easy to design but

the radiation performance is limited due to the lack of enough degrees of design freedom.

This article focuses on the synthesis of unequally spaced planar arrays which is a highly nonlinear and nonconvex problem. Some stochastic optimization methods such as genetic algorithm in [22], particle swarm optimization in [23], invasive weed optimization (IWO) in [24], and others [25], [26] would be potentially suitable due to their ability of escaping from locally optimal solutions. However, when applied to optimize unequally spaced planar array layouts with the minimum element spacing constraint, all of them face the following two challenging problems.

- 1) In each individual updating, all the element spacings between every two neighboring elements over the whole elements should be calculated to determine whether the offspring individual meets the prescribed minimum element spacing constraint. This should be done for each offspring individual of the population. Due to the randomness in the production of offspring individuals, many of the offsprings may fail to meet this constraint.
- 2) These stochastic optimization algorithms are very time-consuming since the performance of every individual at each updating should be evaluated which involves the computation of a huge number of 2-D patterns in a planar array case. Consequently, they are in general suited for small-size arrays, typically less than 100 elements.

For the first problem mentioned above, some techniques such as the modified genetic algorithm (MGA) in [27] and the differential evolution with matrix mapping (DE-MM) in [28] have been presented by simplifying the minimum element spacing constraint as a Chebychev distance constraint in the x - and y -directions separately. Although the Chebychev distance constraint is much easier to process, it cannot guarantee that the produced element positions always meet the original minimum spacing requirement [29]. Recently, an asymmetric mapping method (AMM) is presented in [29] to solve this problem. The DE with asymmetric mapping method (DE-AMM) enhances the restriction on each element in y -direction to guarantee the array meeting the minimum element spacing constraint. However, this method increases the number of the optimization variables which leads to significant increase in both computational and storage loads. As for the second problem, some self-similar structures such as the rotation symmetry in [30] and aperiodic tilings in [31] are exploited to reduce the variables to be optimized so as to significantly save time but at the cost of sacrificing some degrees of synthesis freedom. To the best of our knowledge, purely using stochastic optimization algorithms to synthesize large unequally spaced planar arrays ($N > 500$) with the minimum element spacing constraint has not been reported in the literature.

In our opinion, the two problems mentioned in the stochastic optimization algorithms are mainly derived from the traditional encoding method where each individual represents one implementation of the whole array layout. To address these problems, we propose a DE algorithm with new encoding

mechanism and Cauchy mutation (DE-NEM-CM). The new encoding mechanism which was presented in [32] for wind farm location optimization is now applied in the antenna array layout optimization problem. In this encoding mechanism, each individual represents only one element position rather than an entire array layout. As a consequence, in each individual updating, only an element position may be moved while other elements remain unchanged, which indicates that only the contribution of one antenna element to the radiation pattern needs to be recalculated, so that the computational time is greatly reduced. Moreover, in such a way, if the previous array meets the minimum element spacing constraint, the new array layout generated by one individual updating is easy to meet this constraint again since only the spacings between the changed element and other unchanged elements need to be verified. In addition, the insufficiency of local search in DE-NEM forces us to introduce Cauchy mutation to improve the exploitation while maintaining the diversity of the population. To validate the effectiveness and efficiency of the proposed DE-NEM-CM, several synthesis experiments including a symmetric rectangle array, a broad-band circular array, and beam-scannable square arrays with different aperture sizes are conducted. The results indicate that the proposed DE-NEM-CM has much better performance in term of the sidelobe level than some state-of-the-art stochastic optimization methods. Importantly, it can effectively synthesize large arrays ($N > 1000$) within acceptable time cost, which is very difficult for other stochastic optimization methods.

II. FORMULATION AND ALGORITHM

A. Problem Description

Let us consider a planar array with N isotropic radiating elements placed on a prescribed region Ω of XOY plane. The array factor can be described as follows:

$$AF(u, v) = \sum_{n=1}^N \dot{I}_n e^{j\beta(x_n u + y_n v)} \quad (1)$$

where $j = \sqrt{-1}$, $\beta = 2\pi/\lambda$ denotes the wavenumber in freedom space, (x_n, y_n) and \dot{I}_n denote the position and the complex excitation of the n th element in the array, respectively. $u = \sin\theta \cos\phi - \sin\theta_0 \cos\phi_0$ and $v = \sin\theta \sin\phi - \sin\theta_0 \sin\phi_0$, where θ and ϕ denote the elevation and azimuth angles, respectively, and (θ_0, ϕ_0) represents the desired beam direction.

In this article, we consider the case of the identical excitation ($\dot{I}_n = 1$ for all elements) and focus on the problem of designing large unequally spaced array layouts with the aim of minimizing the peak sidelobe level (PSL), which is the maximum pattern value in the sidelobe region outside of the mainlobe region. In addition, the minimum element spacing constraint is adopted to avoid some nonrealizable solutions. Thus, the concerned synthesis problem can be formulated as

follows:

$$\min_{\vec{x}, \vec{y}} \max_{(u, v) \in \Theta_{SL}} |AF(u, v)|$$

$$\text{Const. } \begin{cases} |AF(u_0, v_0)| = 1, \quad (x_n, y_n) \in \Omega \\ \sqrt{(x_{n_1} - x_{n_2})^2 + (y_{n_1} - y_{n_2})^2} \geq d_{\text{const}} \\ \forall n_1, n_2, \quad n \in \{1, 2, \dots, N\}, \quad n_1 \neq n_2 \end{cases} \quad (2)$$

where $\vec{x} = [x_1, x_2, \dots, x_N]$ and $\vec{y} = [y_1, y_2, \dots, y_N]$, N denotes the number of elements, Θ_{SL} denotes the sidelobe region of array pattern in uv space, d_{const} denotes the required minimum element spacing and Ω represents the prescribed array placement region that is typically a rectangular or circular region.

B. Proposed DE-NEM-CM

The problem in (2) is highly nonlinear and nonconvex. Stochastic optimization methods would be suitable to solve this problem due to their good global search ability. DE algorithm introduced in [33] is one of the most popular swarm-based optimizers, and DE and its variants have been widely applied to solve array synthesis problems [34]–[36]. To solve Problem (2), DE-NEM-CM is proposed in this article.

1) New Encoding Mechanism: For Problem (2), the traditional encoding mechanism is that an individual, denoted as $\vec{X}_i = [x_1, y_1, x_2, y_2, \dots, x_N, y_N]$ ($i \in \{1, 2, \dots, NP\}$ where NP denotes the population size), represents an array layout, shown in Fig. 1(a). With such a encoding mechanism, all the spacings between neighboring elements in an individual should meet the prescribed minimum element spacing constraint in (2). However, this is very difficult for an arbitrary offspring individual which is generated by evolution operators in the stochastic optimization methods such as DE. If offspring individuals always fail to meet the prescribed minimum element spacing constraint, the evolution process will stagnate. Some techniques such as AMM in [29] can be incorporated into the evolution process to generate layout candidates meeting the minimum element spacing constraint. However, these techniques significantly increase the dimension of the problem and are unsuitable for large array layout optimization problems as mentioned in the Introduction.

To overcome the mentioned problem, a new encoding mechanism which was used in [32] to optimize wind farm layout is adopted. In this encoding mechanism, an individual denoted as $\vec{X}_i = [x_i, y_i]$ ($i \in \{1, 2, \dots, N\}$) represents only a certain element position, and the whole population denoted as $\mathbf{P} = \{[x_1, y_1], [x_2, y_2], \dots, [x_N, y_N]\}$ represents an array layout. The difference between the traditional and new encoding mechanisms is intuitively shown in Fig. 1. With new encoding mechanism, the variation of an individual may lead to the position updating for only one element in the array. Hence, when the initial array meets the minimum element spacing constraint, the probability that the variation of an offspring individual leads to a failure to meet the minimum element spacing constraint is much lower than that with the traditional encoding mechanism, which will significantly reduce the possibility of the stagnation of the evolution process. Furthermore, in each individual updating,

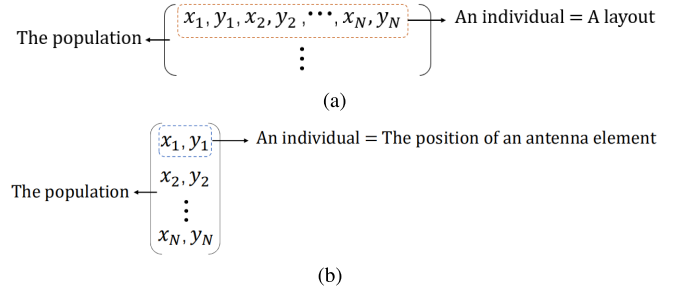


Fig. 1. Difference between the traditional and new encoding mechanism. (a) Traditional encoding mechanism. (b) New encoding mechanism.

the contribution of one antenna element to the array pattern needs to be recalculated, while the main part of array pattern from all the other elements remains unchanged, which greatly reduces the computational time and complexity. In addition, the search space for each individual always maintains in two dimensions regardless of the number of antenna elements. As is well known, the low-dimension search space facilitates the algorithm to quickly find the best solution.

2) Evolution Strategies: In the proposed DE-NEM-CM, we utilize some strategies including the mutation, crossover, replacement, and selection to evolute the population. Particularly, the replacement mechanism is absent from the traditional DE, and it is adopted to improve the diversity of the population for catering to the new encoding mechanism.

a) Mutation: For each target individual \vec{X}_i in the population, the corresponding mutation individual \vec{V}_i is generated by utilizing the mutation operator, which is given by

$$\vec{V}_i = \vec{X}_{r_1} + F \cdot (\vec{X}_{r_2} - \vec{X}_{r_3}), \quad i = 1, 2, \dots, N \quad (3)$$

where random indexes $r_1, r_2, r_3 \in \{1, 2, \dots, N\}$ are mutually different integers and also different from index i , $F > 0$ is a scaling factor, and $(\vec{X}_{r_2} - \vec{X}_{r_3})$ is a difference vector. It is noteworthy that the information of three mutually different individuals is utilized to guide the generation of the mutation individual, which focuses on the exploration.

b) Crossover: To generate the multifarious trial individual, the crossover operator is used. For each pair of \vec{X}_i and \vec{V}_i , the crossover individual \vec{U}_i is generated via the following way:

$$U_{i,d} = \begin{cases} V_{i,d}, & \text{if } \text{rand}_d(0, 1) < CR \text{ or } d = d_{\text{rand}} \\ X_{i,d}, & \text{otherwise} \end{cases} \quad (4)$$

where $i = 1, 2, \dots, N$, $d = 1, 2$, $\text{rand}_d(0, 1)$ denotes an uniform random number in the interval $[0, 1]$, $CR \in [0, 1]$ denotes the crossover constant, and $d_{\text{rand}} \in \{1, 2\}$ represents a randomly selected dimension index.

c) Replacement: After successively implementing mutation and crossover operators, we obtain an offspring population \mathbf{Q} which consists of the crossover individual \vec{U}_i ($i = 1, 2, \dots, N$). Especially, the first offspring individual in \mathbf{Q} randomly replaces a parent individual in \mathbf{P} , which is regarded as an individual updating. The updated \mathbf{P} is obviously an new population denoted as \mathbf{S} . Since the problem in (2) involves the minimum element spacing constraint, we firstly should check whether \mathbf{S} meets this constraint. If \mathbf{S} meets the constraint,

the better one between \mathbf{P} and \mathbf{S} is determined and retained via the following selection operator, then the remaining offspring individuals in \mathbf{Q} one by one will accomplish the replacement and selection with same procedures as the first offspring individual.

d) Selection: According to the problem in (2), we use the PSL as the fitness function in the proposed DE-NEM-CM shown in the following:

$$f(\mathbf{P}) = \max_{(u,v) \in \Theta_{\text{SL}}} |AF(u,v)|. \quad (5)$$

Obviously, the fitness function value is determined by the whole population \mathbf{P} rather than a certain individual, which is different from the traditional DE. The selection operator is applied to determine the better one between the population \mathbf{P} and \mathbf{S} based on the fitness function $f(\cdot)$ in (5), and the better one will survive into the next updating. The selection mechanism is described as

$$\mathbf{P}' = \begin{cases} \mathbf{S}, & \text{if } f(\mathbf{S}) < f(\mathbf{P}) \\ \mathbf{P}, & \text{otherwise.} \end{cases} \quad (6)$$

3) Cauchy Mutation: Note that new encoding mechanism renders only the position of one element in the array being moved in an individual updating, similar to the local search of greedy algorithm, which is poor at the exploration. Nevertheless, the generation and random replacement mechanisms of offspring individuals in the above evolution strategies mainly focus on the exploration. Hence, DE with new encoding mechanism can well integrate their advantages. However, the inherent local search characteristic on new encoding mechanism is not enough to obtain a satisfactory synthesis result. Thus, Cauchy mutation with chaotic mapping is incorporated into the selection operator of the evolution process mentioned above to enhance the local search while maintaining the diversity of population.

In above selection operator, if \mathbf{P} is successfully replaced by \mathbf{S} , the newly retained offspring individual in \mathbf{P} is denoted as X'_i , and its vicinity is regarded to have the potential to provide better radiation performance. Thus, this individual will be further exploited to generate new offspring individual X''_i by using Cauchy mutation with chaotic mapping, which is described as

$$X''_{i,d} = X'_{i,d} + c_k \cdot \delta_d, \quad d = 1, 2 \quad (7)$$

where random variable $\delta_d \sim C(0, 1)$, which represents the standard Cauchy distribution [37]. The chaotic sequence $\{c_k\}$ is generated by the following equation [38]:

$$c_{k+1} = \mu \cdot c_k \cdot (1 - c_k), \quad \mu \in [0, 4] \quad (8)$$

where k denotes the number of generation, the original state c_1 is equal to 0.01. μ denotes the logistic parameter and equals to 4, which makes the system being in chaotic state.

Then new offspring individual X''_i will replace X'_i in \mathbf{P} to constitute the new population \mathbf{S}' , and the selection operator is applied to \mathbf{P} and \mathbf{S}' . Obviously, this Cauchy mutation enhances the local search ability of DE with new encoding mechanism. Due to the long flat tails of Cauchy

density function, Cauchy mutation is more likely to generate an offspring individual further away from its parent than Gaussian mutation [39]. Furthermore, an adaptive search step size generated by chaotic mapping in (8) contributes to maintaining the diversity of the population due to the ergodicity of chaotic variable. Therefore, the proposed DE-NEM-CM can well balance the exploitation and exploration.

C. DE-NEM-CM Synthesis Procedure

In the initialization of the proposed DE-NEM-CM, \mathbf{P} is generated by selecting randomly N element positions in a fully filled array, which is a fast and simple way to generate a large unequally spaced planar array that meets the prescribed minimum element spacing constraint. Then the contribution of each element to the array pattern will be calculated and stored, and the PSL of \mathbf{P} is calculated by (5). During the evolution, the mutation operator in (3) and crossover operator in (4) are successively implemented on parent individual $\vec{X}_i = [x_i, y_i]$ in \mathbf{P} to generate offspring individual denoted as $X'_i = [x'_i, y'_i]$, where $i = 1, 2, \dots, N$. This naturally forms an offspring population $\mathbf{Q} = \{[x'_1, y'_1], [x'_2, y'_2], \dots, [x'_N, y'_N]\}$, then the first offspring individual X'_1 in \mathbf{Q} will randomly replace a parent individual in \mathbf{P} , the updated \mathbf{P} is denoted as a new population \mathbf{S} . Then \mathbf{S} is checked whether meeting the constraints in (2). If \mathbf{S} meets these constraints, the corresponding PSL is calculated by (5). Moreover, if \mathbf{S} provides a lower PSL than \mathbf{P} , \mathbf{P} is replaced by \mathbf{S} ; otherwise, \mathbf{P} keeps unchanged. Especially, if \mathbf{P} is successfully replaced by \mathbf{S} , Cauchy mutation in (7) will be implemented on this offspring individual to generate new offspring individual denoted as $X''_1 = [x''_1, y''_1]$. Afterward, new individual X''_1 tries to replace X'_1 while other individuals keep unchanged, forming a new population \mathbf{S}' . If \mathbf{S}' meets the constraints in (2), the corresponding PSL is calculated. By comparing the PSLs between \mathbf{P} and \mathbf{S}' , we reserve the one with lower PSL. Subsequently, the above process is implemented on the remaining individuals in \mathbf{Q} one by one until the user-defined maximum number of FEs (*MaxFEs*), shown as **Algorithm 1**.

III. NUMERICAL EXPERIMENTS

To validate the effectiveness and robustness of the proposed DE-NEM-CM method, we will conduct a set of examples for synthesizing different unequally spaced planar array layouts including a symmetric rectangular array, a broadband circular array as well as beam-scannable square arrays with varying apertures. In all examples, we choose scaling factor $F = 0.5$ and crossover constant $CR = 0.9$, and the population size NP is just equal to the number of elements N . The required minimum element spacing d_{const} is set as 0.5λ which is a typical choice in conventional antenna array designs. All the synthesis experiments are executed on the same computer with Intel Xeon E5-2697 CPU and 512 GB memory.

A. Sparse Rectangular Array

As the first example, we will synthesize a sparse rectangular array with $4N$ elements on an aperture of $9.5\lambda \times 4.5\lambda$. This

Algorithm 1 DE-NEM-CM Synthesis Procedure

```

1: Set the number of elements  $N$ , scaling factor  $F$ , crossover
   constant  $CR$ , and maximum number of fitness eval-
   uations (FEs)  $MaxFEs$ , the required minimum element
   spacing  $d_{\text{const}}$ ;
2: The positions of  $N$  elements randomly selected from a
   fully filled array are regarded as the initial population
   denoted as  $\mathbf{P} = \{[x_1, y_1], [x_2, y_2], \dots, [x_N, y_N]\}$ , where
   each individual  $\vec{X}_i = [x_i, y_i]$  represents an element position,
    $i = 1, 2, \dots, N$ ;
3:  $FEs = 0$ ;
4: Calculate the PSL of  $\mathbf{P}$  by (5) and set  $k = 0$ ;
5: while  $FEs < MaxFEs$  do
6:   Count  $k = k + 1$ ;
7:   Generate offspring population which is denoted as
       $\mathbf{Q} = \{[x'_1, y'_1], [x'_2, y'_2], \dots, [x'_N, y'_N]\}$  by implementing
      the
      mutation operator in (3) and crossover operator in (4) on
      each
      individual  $\vec{X}'_i$ ,  $i = 1, 2, \dots, N$ .
8:   for  $i = 1$  to  $N$  do
9:     Offspring individual  $\vec{X}'_i = [x'_i, y'_i]$  in  $\mathbf{Q}$  randomly
      replaces
      an individual in  $\mathbf{P}$ , and the updated  $\mathbf{P}$  is denoted as  $\mathbf{S}$ ;
10:    if  $\mathbf{S}$  meets the constraints in (2) then
11:      Calculate the PSL of  $\mathbf{S}$  by (5);
12:       $FEs = FEs + 1$ ;
13:      if  $\mathbf{S}$  provides lower PSL than  $\mathbf{P}$  then
14:         $\mathbf{P} = \mathbf{S}$ ;
15:        Generate offspring individual  $\vec{X}''_i = [x''_i, y''_i]$  by
          utilizing Cauchy mutation in (7) on  $\vec{X}'_i$ , and the
          individual  $\vec{X}''_i$  will replace  $\vec{X}'_i$  in  $\mathbf{P}$ , forming
          a new population  $\mathbf{S}'$ ;
16:        if  $\mathbf{S}'$  meets the constraints in (2) then
17:          Calculate the PSL of  $\mathbf{S}'$  by (5);
18:           $FEs = FEs + 1$ ;
19:          if  $\mathbf{S}'$  provides lower PSL than  $\mathbf{P}$  then
20:             $\mathbf{P} = \mathbf{S}'$ ;
21:            end if
22:          end if
23:        end if
24:      end if
25:    end for
26:  end while
27: return  $\mathbf{P}$ 

```

array is placed in XOY plane and its layout is symmetric about both x -axis and y -axis. In view of its symmetry, only a quarter of element positions in this array (i.e., N elements) needs to be optimized. It is noteworthy that the minimum element constraint is taken into account in this article. Assume that a broadside beam pattern is desired. This example was synthesized by the MGA in [27], the DE-MM in [28], and the DE-AMM in [29]. The three methods adopted the same settings for the key parameters: $d_{\text{const}} = 0.5\lambda$, $N = 25$, $NP = 100$, and maximum generations of 300. That is, the maximum

TABLE I

PERFORMANCE COMPARISON BETWEEN THE PROPOSED DE-NEM-CM AND SOME STATE-OF-THE-ART ALGORITHMS FOR A SPARSE RECTANGULAR ARRAY OCCUPYING AN APERTURE OF $9.5\lambda \times 4.5\lambda$

Algorithm	N	$MaxFEs$	K	Performance		
				TNM / 10^{10}	Lowest PSL (dB)	Mean PSL (dB)
IWO [24]	23	27500	5	6.3	-21.20	-
MGA [27]	25	30000	5	7.5	-18.84	-
DE-MM [28]	25	30000	5	7.5	-20.38	-
DE-AMM [29]	25	30000	100	150.0	-21.88	-
DE-NEM	23	10000	100	2.0	-22.11	-19.71
DE-NEM-CM	23	10000	100	2.0	-23.33	-20.87

number of FEs ($MaxFEs$) for each trial is 30000. The array pattern in the optimization process was calculated with $M = 100 \times 100$ samples in the (u, v) -space within the region of $0 \leq u, v \leq 1$. They were performed with 5, 5, and 100 trials, respectively. The lowest PSLs obtained by the three methods in all trials were -18.84 , -20.38 , and -21.88 dB, respectively. Besides, the IWO in [24] also considered the same example but with $N = 23$, maximum plants of 55, and maximum iterations of 500, which means that $MaxFEs$ is equal to 27500. Furthermore, the obtained lowest PSL among 5 trials was -21.20 dB. As we known the main time cost for these methods is spent on a large number of repeated evaluations of the array pattern which involves the calculation of the inner product between the discretized observation direction vector $[u_m, v_m]$ (for $m = 1, 2, \dots, M$) and the position vector $[x_n, y_n]$ (for $n = 1, 2, \dots, N$) in (1). The total number of multiplications (TNM) for K trials is about $2M \times N \times MaxFEs \times K$. Some statistic results for these methods are listed in Table I.

Here we apply the proposed DE-NEM-CM to synthesize the same example with the parameters $d_{\text{const}} = 0.5\lambda$, $N = 23$, $F = 0.5$, $CR = 0.9$, and $MaxFEs = 10000$. The array pattern evaluation is performed on the same M samples within the region of $0 \leq u, v \leq 1$ for comparison. As a result, we uniformly sample 100 points for ϕ from 0° to 90° as well as θ from 0° to 90° . It is worth noting that, for all examples in this article, we use the seeded region growing in [40] to determine the mainlobe region of the pattern. Once determining the mainlobe region, we can identify the sidelobe region and then obtain the PSL. One hundred trials are used in this example. In all these trials, the obtained lowest and mean PSLs are -23.33 and -20.87 dB, respectively. Clearly, the lowest PSL obtained by the proposed DE-NEM-CM is much lower than those obtained by the methods mentioned above. Fig. 2(a) and (b) show a quarter of the array pattern for the trial with the lowest PSL and its three cuts at $\phi = [0^\circ, 45^\circ, 90^\circ]$, respectively. A quarter of the corresponding array layout (the symbol ‘.’ denotes an antenna element) is shown in Fig. 3, and the coordinates for all the element positions shown in Fig. 3 is given in Table II where two decimals are reserved. It can be confirmed that the minimum

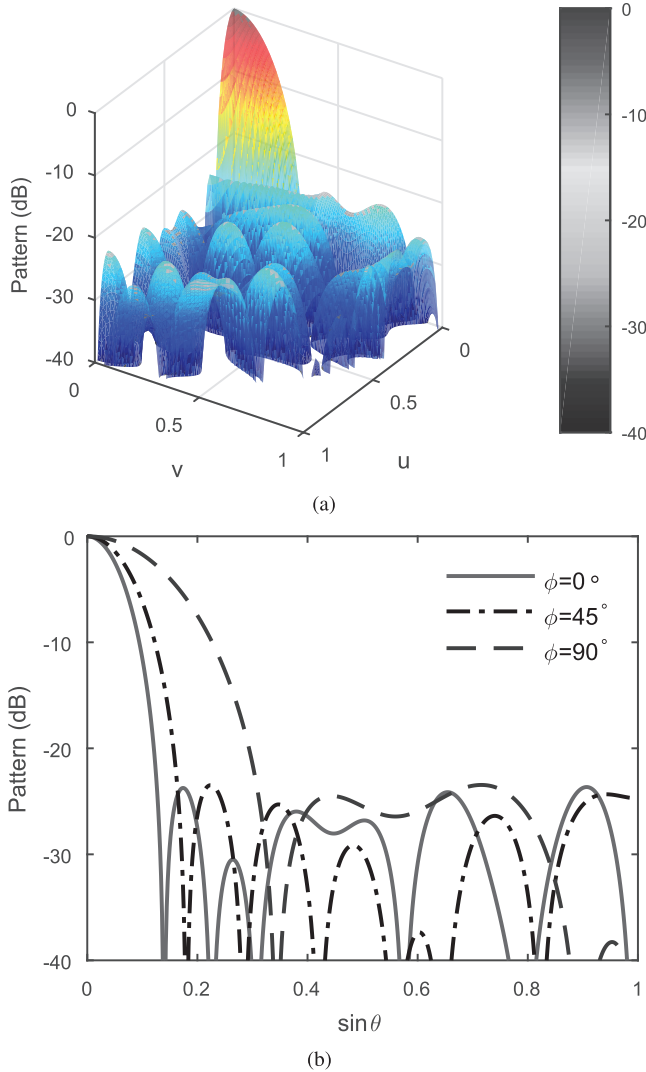


Fig. 2. Array pattern obtained by the proposed DE-NEM-CM at the best trial. (a) Quarter pattern. (b) Three cuts of the quarter pattern at $\phi = 0^\circ$, 45° , and 90° .

element spacing between arbitrary two elements is no less than 0.5λ as is expected.

To validate the effectiveness of the Cauchy mutation used in the selection operator of the proposed DE-NEM-CM, we apply the DE-NEM (without the Cauchy mutation) to synthesize this example, and the same parameter settings and number of trials as the proposed DE-NEM-CM are used. The PSLs obtained by the DE-NEM and the proposed DE-NEM-CM versus the number of FEs for different trials are depicted in Fig. 4(a) and (b), respectively. It is noteworthy that the lowest PSL obtained by DE-NEM for all trials are -22.11 dB, which is higher than -23.33 dB in the proposed DE-NEM-CM. Moreover, the obtained mean PSL is -19.71 dB which is also worse than -20.87 dB in the proposed DE-NEM-CM. The comparison directly validates the effectiveness of the Cauchy mutation in the proposed DE-NEM-CM. Due to the application of new encoding mechanism, the proposed DE-NEM-CM and DE-NEM only need to calculate the inner product between the discretized observation direction vector $[u_m, v_m]$ (for $m = 1, 2, \dots, M$) and one element position in each individual

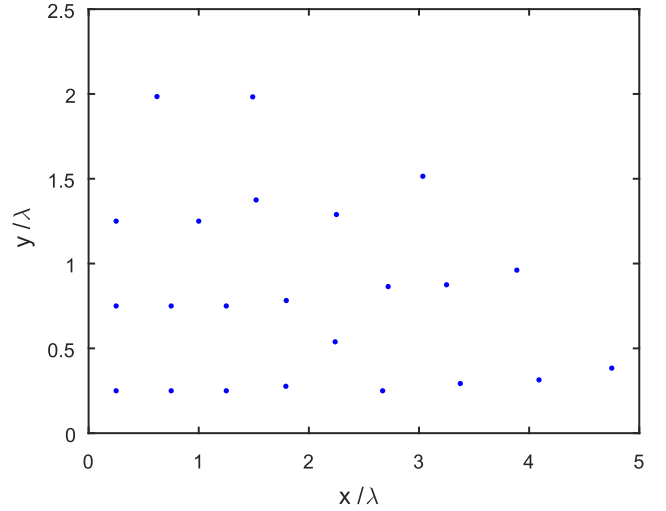


Fig. 3. Quarter of the best array layout obtained by the proposed DE-NEM-CM in all trials.

TABLE II
ELEMENT COORDINATES OF THE QUARTER OF THE BEST ARRAY LAYOUT
OBTAINED BY THE PROPOSED DE-NEM-CM IN WAVELENGTH, n :
 (x_n, y_n) , WHERE TWO DECIMALS ARE RESERVED

1: (0.25,0.25)	2: (0.75,0.25)	3: (1.25,0.25)	4: (2.66,0.25)
5: (1.79,0.27)	6: (3.37,0.29)	7: (4.08,0.31)	8: (4.74,0.38)
9: (2.23,0.53)	10: (0.25,0.75)	11: (0.75,0.75)	12: (1.25,0.75)
13: (1.79,0.78)	14: (2.71,0.86)	15: (3.25,0.87)	16: (3.88,0.96)
17: (0.25,1.25)	18: (1.00,1.25)	19: (2.25,1.28)	20: (1.52,1.37)
21: (3.03,1.51)	22: (0.62,1.98)	23: (1.49,1.98)	

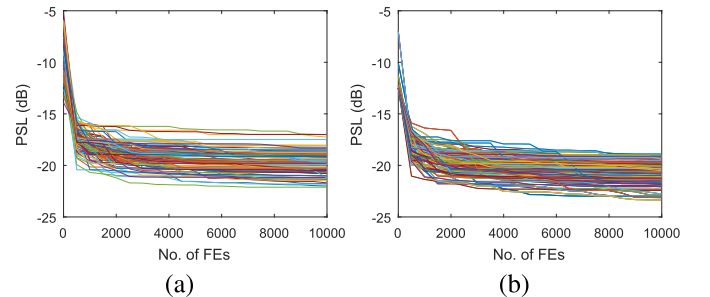


Fig. 4. Convergence curves on the PSL obtained by (a) DE-NEM and (b) proposed DE-NEM-CM, for 100 trials.

updating. Hence, their TNM for the evaluations of the array pattern in (1) are estimated as $2M \times \text{Max FEs} \times K$. Statistic results for these two methods are also recorded in Table I.

From the comparison between the proposed DE-NEM-CM and these state-of-the-art algorithms mentioned above in Table I, we observe that, although the number of trials performed by the proposed DE-NEM-CM and DE-NEM are 100 which is equal to or more than other algorithms, the TNMs of these two algorithms are least one among these methods, which indicates that the cost time is least. Therefore, the proposed DE-NEM-CM applies the least total multiplications and the number of elements to obtain the lowest PSL, which adequately shows the effectiveness and efficiency of the proposed DE-NEM-CM.

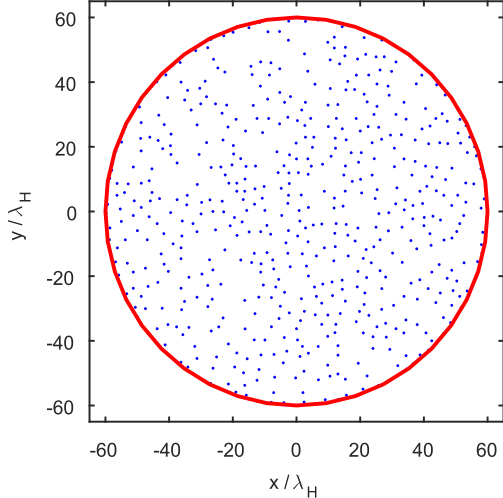


Fig. 5. Broadband circular sparse array layout obtained by the proposed DE-NEM-CM at the best trial.

B. Broadband Circular Sparse Array

In the second example, we will check the effectiveness and superiority of the proposed DE-NEM-CM for synthesizing a broadband circular sparse array layout. In this case, all the elements are located in a prescribed circular area. That is, the element positions are bounded with $\sqrt{x_n^2 + y_n^2} \leq R$ ($n = 1, 2, \dots, N$) where R denotes the radius of circular area.

In [31], a perturbed Penrose tiling array working in $f_H/f_L = 5:1$ frequency bandwidth was designed by GA with 551 elements on a circular aperture of $R = 12\lambda_L = 60\lambda_H$ where λ_L and λ_H are the wavelengths at the lowest frequency f_L and the highest frequency f_H , respectively. The minimum element spacing constraint was taken as $d_{\text{const}} = 0.5\lambda_L = 2.5\lambda_H$. In the GA perturbation, 150 generations with 50 individuals for the population size were carried out to reach the convergence. The obtained lowest PSL was -10.35 dB at the highest frequency f_H and -16.64 dB at the lowest frequency f_L . Although the Penrose tiling array combining with GA perturbation in [31] achieves much better performance than a conventional uniformly spaced array in terms of broadband PSL and GLL suppression for the sparse array, the obtained pattern performance is restricted by the Penrose tiling array representation.

In this example, we apply the proposed DE-NEM-CM to reoptimize this array for further reducing the broadband PSL and GLL. For comparison, we adopt the same settings in the element number, the minimum element spacing, and the total aperture as those used in [31]. The number of FEs is set as $\text{MaxFES} = 20\,000$ in this example. To avoid the presence of grating lobes, the array performance is optimized at the highest frequency f_H . Generally, for the case of the equally spaced array with uniform excitations, we uniformly sample ϕ from 0° to 180° as well as θ from -90° to 90° , and set the sampling density as $\Delta\theta = \Delta\phi = \lambda/(10D_{\max})$, where D_{\max} denotes the maximum array aperture. Such a sampling manner indicates that there exists 20 sampling points within the first null beamwidth (FNBW) of the pattern and the FNBW

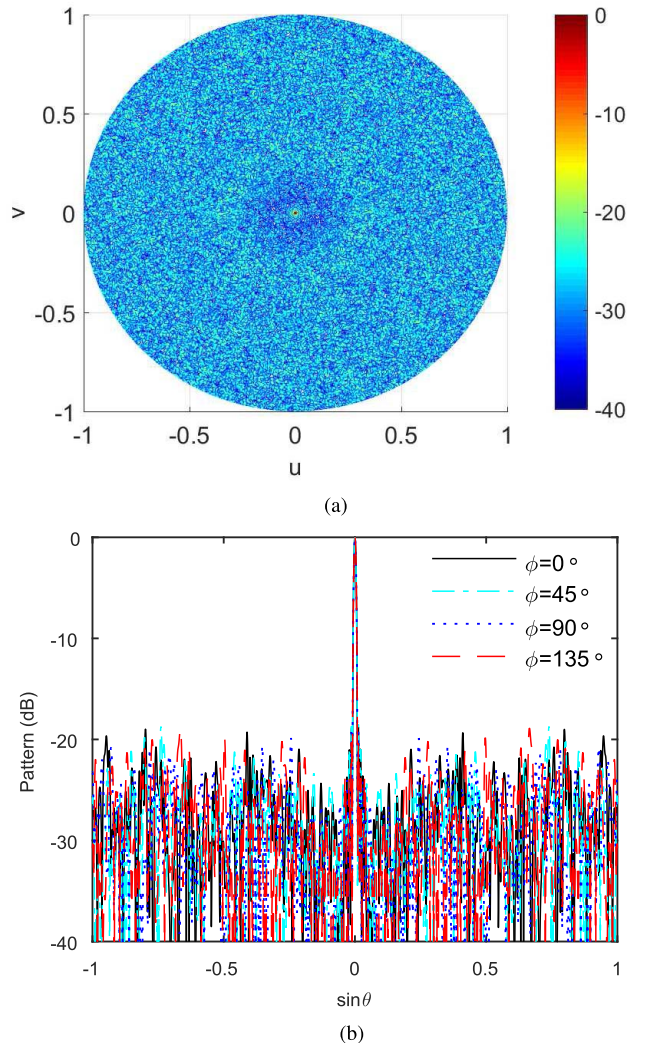


Fig. 6. Array pattern obtained by the proposed DE-NEM-CM at the highest frequency f_H over the whole 5:1 frequency bandwidth. (a) Top view of the synthesized pattern in (u, v) plane. (b) Cuts of the array pattern at $\phi = 0^\circ, 45^\circ, 90^\circ$, and 135° .

is approximately equal to $2\lambda/D_{\max}$. Taking the sampling rule mentioned above as a reference, we set $\Delta\theta = \Delta\phi = 0.05^\circ$ for the ultrabroadband array in this example. Five trials are used in the proposed DE-NEM-CM. The obtained lowest and mean PSLs are -18.35 and -18.21 dB, respectively. The array layout for the best trial with the lowest PSL is shown in Fig. 5. It can be checked this array layout meets both the minimum element spacing constraint and as the aperture boundary as indicated by the red circle in Fig. 5. The obtained average element spacing reaches about $4.53\lambda_H$. Fig. 6(a) and 6(b) show the top view of the corresponding array pattern and its four cuts at the highest frequency f_H , respectively. The obtained PSL at f_H is -18.35 dB which is much lower than -10.35 dB that is obtained in [31]. Fig. 7(a) and (b) show the top view of the corresponding pattern and its four cuts at the lowest frequency f_L , respectively. The PSL at f_L is -18.48 dB which is also considerably lower than -16.64 dB that is obtained in [31]. This indicates that the proposed DE-NEM-CM can achieve much better performance than the method by combining the Penrose tiling representation and

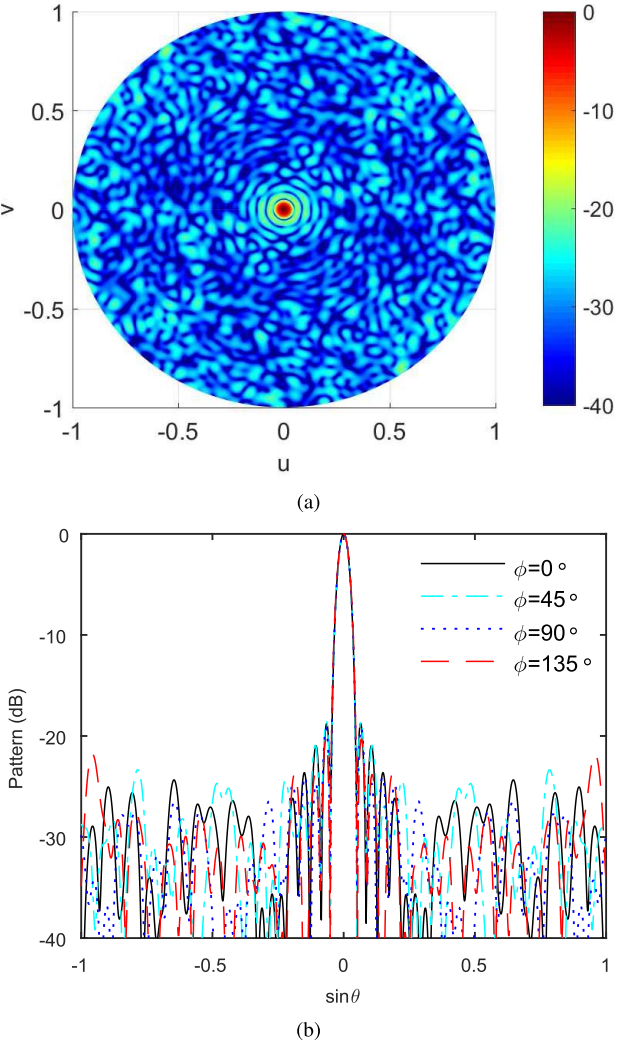


Fig. 7. Array pattern obtained by the proposed DE-NEM-CM at the lowest frequency f_L over the whole 5:1 frequency bandwidth. (a) Top view of the synthesized pattern in (u, v) plane. (b) Cuts of the array pattern at $\phi = 0^\circ, 45^\circ, 90^\circ$, and 135° .

GA perturbation for suppressing both the PSL and GSL of a broadband sparse array.

In this example, if we adopt $\lambda_L/2$ -spaced elements occupying the same circular area with $R = 12\lambda_L$, a total of 1804 elements would be required. Compared with this uniformly spaced array, the synthesized sparse array layout can save about 69.46% elements. The element saving can be even as high as 98.78% if compared with a $\lambda_H/2$ -spaced array occupying the same circular area (since a $\lambda_L/2$ -spaced planar array will have a number of grating lobes in high-frequency band). Such an ultrasparse array is useful when a narrow radiation beam is required over a ultrawideband such as in radio astronomy application.

C. Beam-Scannable Sparse Square Arrays With Varying Aperture Sizes

In the last example, we will synthesize beam-scannable sparse square arrays with varying sizes to check the robustness of the proposed DE-NEM-CM method. We consider five sizes of sparse square arrays, and some parameters including

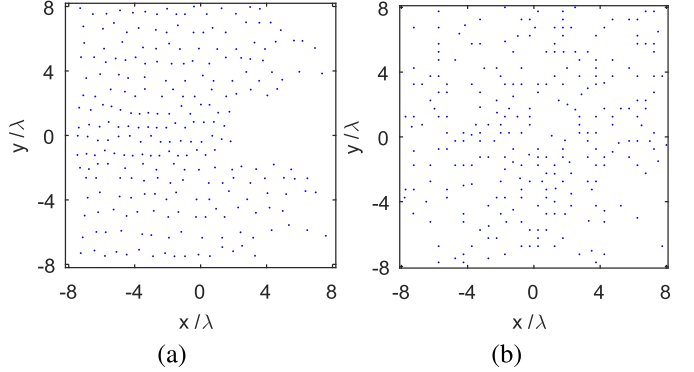


Fig. 8. 256-element array layouts obtained by (a) DE-AMM and (b) proposed DE-NEM-CM, at their best trials.

the aperture sizes, the number of elements (N), and filling factors (FFs) (which is defined as the ratio of the number of elements for the sparse array to the one for a $\lambda/2$ -spaced array occupying the same aperture) are given in Table III.

Assume that for all sizes of arrays, the beam pointing direction can be scanned from $\theta_0 = -45^\circ$ to 45° for an arbitrary ϕ_0 , i.e., $\theta_0 \in [-45^\circ, 45^\circ]$ and $\phi_0 \in [0, 360^\circ]$. In this situation, the array layout can be still optimized by evaluating a broadside beam pattern performance but in an enlarged (u, v) -space given by $\sqrt{u^2 + v^2} \leq 1 + \sin 45^\circ$. According to the sampling rule mentioned in the second example, we set different sampling density $\Delta\theta = \Delta\phi$ for the above-mentioned five arrays and, respectively, record them in Table III. The maximum number of FEs is set as $MaxFEs = 100N$. The proposed DE-NEM-CM is performed 5 trials for each size of array layout optimization. In addition, we also apply the DE-AMM in [29] to synthesize all these sizes of arrays for comparison. Furthermore, the same sampling densities as the proposed DE-NEM-CM are used for these arrays. In the DE-AMM, the optimization of element positions is transformed into the optimization of variable matrices A , B , and W which are defined in [29], and the size of these matrices is determined by G and J which are obtained by solving the problem (2) in [29]. If $G \times J = N$, weight matrix W is eliminated, so the search dimension of each individual is equal to $2G \times J + G + J$. Otherwise, the search dimension is equal to $3G \times J + G + J$. Therefore, as N increases from 64 to 1024, the dimension of each individual in DE-AMM is 144, 413, 544, 1630, and 2112, respectively. However, the dimension of each individual in the proposed DE-NEM-CM is always equal to 2 regardless of the array size. With the parameters $NP = 3N$ for the population size, $F = 0.5$ and $CR = 0.9$, the DE-AMM is executed 5 trials as well, and 2000 iterations is performed for each trial. Table III lists the synthesis results by the proposed DE-NEM-CM and the DE-AMM, including the achievable lowest and mean PSL over five trials, the half power beamwidth (HPBW) (the widest one among the HPBWs for different cuts of the pattern at the best trial), and the average time cost over five trials.

From the results shown in Table III, we can see that for the cases of 64, 128, and 256 elements, the proposed DE-NEM-CM can take much less time cost to obtain a sparse array layout with a considerably lower PSL and the mean PSL over

TABLE III
PERFORMANCE COMPARISON BETWEEN THE PROPOSED DE-NEM-CM AND THE DE-AMM IN [29] FOR BEAM-SCANNABLE SQUARE ARRAYS WITH DIFFERENT APERTURE SIZES

Aperture	N	Filling factors (%)	$\Delta\theta = \Delta\phi$ (°)	DE-AMM				The proposed DE-NEM-CM			
				HPBW (°)	Mean PSL (dB)	Lowest PSL (dB)	Time (h)	HPBW (°)	Mean PSL (dB)	Lowest PSL (dB)	Time (h)
$6\lambda \times 6\lambda$	64	44.44	0.9	8.00	-10.84	-12.41	10.96	8.00	-13.88	-14.38	0.07
$10\lambda \times 10\lambda$	128	32.00	0.5	4.56	-14.45	-14.83	84.58	5.00	-15.96	-16.18	0.53
$16\lambda \times 16\lambda$	256	25.00	0.35	2.82	-	-15.18	597.20	2.80	-18.16	-18.28	4.30
$26\lambda \times 26\lambda$	512	18.93	0.2	-	-	-	-	1.60	-20.29	-20.46	19.22
$42\lambda \times 42\lambda$	1024	14.51	0.14	-	-	-	-	1.08	-22.23	-22.32	93.41

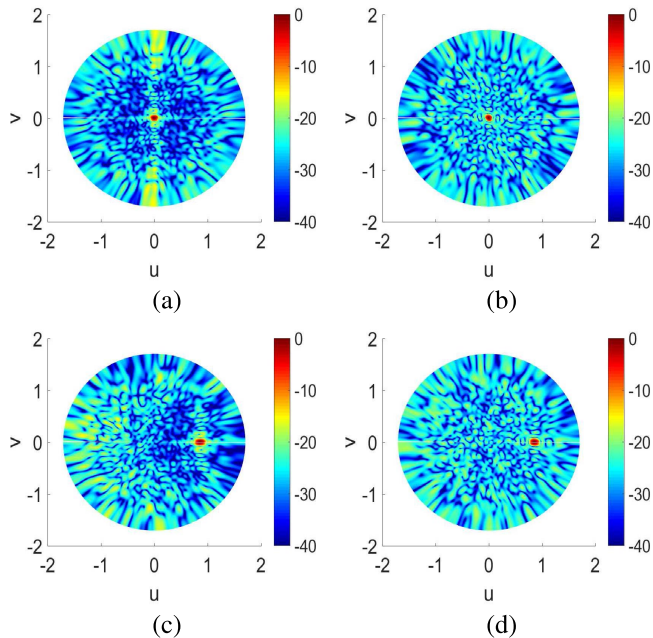


Fig. 9. Top views of broadside beam patterns obtained by (a) DE-AMM and (b) proposed DE-NEM-CM, and the top views of two patterns with the beam direction of $(\theta_0, \phi_0) = (45^\circ, 0^\circ)$ obtained by (c) DE-AMM and (d) proposed DE-NEM-CM.

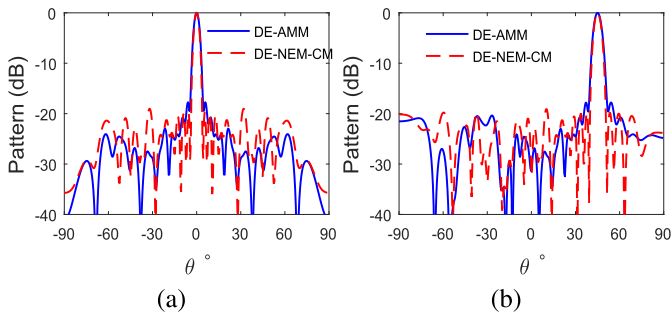


Fig. 10. Comparison between the DE-AMM and the proposed DE-NEM-CM on the $\phi = 0^\circ$ cuts of (a) broadside beam patterns and (b) beam patterns scanned to direction $(\theta_0, \phi_0) = (45^\circ, 0^\circ)$.

five trials than the DE-AMM. For example, for the case of 256-element array, the proposed DE-NEM-CM takes the average time of 4.30 h to obtain a sparse array with the lowest PSL of -18.28 dB and the mean PSL of -18.16 dB, while the DE-AMM takes 597.20 h for obtaining a result with a PSL of -15.18 dB. It is worth noting that the 597.20 h for the DE-AMM is the time cost of one trial since we cannot bear to

perform five trials for such time consumption. Fig. 8(a) and (b) show the 256-element array layouts obtained by the DE-AMM and the proposed DE-NEM-CM, respectively. Fig. 9(a) and (b) show the top views of broadside beam patterns radiated by these two arrays, and Fig. 9(c) and (d) show the top views of two beam patterns scanned to the direction of $(\theta_0, \phi_0) = (45^\circ, 0^\circ)$. Furthermore, the comparison between the DE-AMM and the proposed DE-NEM-CM on the $\phi = 0^\circ$ cuts of broadside beam patterns is shown in Fig. 10(a), and the case of beam patterns scanned to the direction of $(\theta_0, \phi_0) = (45^\circ, 0^\circ)$ is also shown in Fig. 10(b). From this comparison, we can intuitively see that the proposed DE-NEM-CM obtains a lower PSL than the DE-AMM.

For larger sizes of arrays with 512 and 1024 elements, the DE-AMM will take terrible time cost and even one trial is not realistic. By contrast, the proposed DE-NEM-CM can still work. For the array with 512 elements, the proposed DE-NEM-CM obtains the lowest PSL of -20.46 dB and the mean PSL of -20.29 dB with average time cost of 19.22 h. For the array with 1024 elements, the obtained lowest PSL and its mean are -22.32 and -22.23 dB with average time cost of 93.41 h, respectively. This means that even for so large array layout optimization, the proposed DE-NEM-CM can still obtain reasonable synthesis results within affordable time cost. Furthermore, the obtained mean PSLs for different array sizes show the good robustness of the proposed DE-NEM-CM. In addition, the comparison between the DE-AMM and the proposed DE-NEM-CM demonstrates the superiority of new encoding mechanism used in the DE-NEM-CM.

IV. CONCLUSION

In this article, we have proposed a DE-NEM-CM to optimize large unequally spaced planar array layouts with the minimum element spacing constraint. The new encoding mechanism adopted in the proposed DE-NEM-CM is that an individual represents only one element position, which is much different from the traditional encoding which uses an individual to represent an entire array layout. With the new encoding mechanism, the proposed optimization algorithm can efficiently evaluate the array pattern in each individual updating by only modifying the radiation contribution from one antenna element associated with the position variation, which greatly reduces the computational complexity. In addition, this encoding mechanism naturally facilitates the array layout candidates to meet the minimum element spacing constraint.

The Cauchy mutation with chaotic mapping is incorporated into the selection operator to enhance the exploitation of the DE-NEM while preserving the diversity of the population. A set of experiments for synthesizing unequally spaced planar arrays with different requirements are conducted. The comparisons with some state-of-the-art stochastic optimization methods are also given in the examples. Results show that the proposed DE-NEM-CM requires much less time cost while maintaining comparable or even better pattern performance compared with conventional stochastic optimization algorithms. In particular, the proposed method is capable of optimizing unequally spaced planar arrays with as many as 1000 elements within acceptable time cost, which is a very challenging problem and rarely reported in the literature. The proposed DE-NEM-CM provides a promising technique to tackle the large unequally spaced array layout optimization problem.

It should be noted that the proposed method is in general useful for geometry optimization of phased antenna arrays where each element is individually excited. This method can be further generalized to deal with the array geometry optimization with different element structures. The effect of an antenna element structure can be considered by multiplying the array factor with the element pattern. However, the mutual coupling effect cannot be included in the current method. One can consider the mutual coupling effect in the element position optimization process by combining some iterative position optimization strategies and full-wave simulation technique. However, such techniques are very time-consuming and they cannot be applied to large unequally spaced array layout optimization problems. On the other hand, since the minimum element spacing constraint is usually set to be no less than half a wavelength, the obtained averaged element spacing is usually much larger than half a wavelength. In this situation, the mutual coupling effect is not very strong, and the array pattern performance without considering mutual coupling can approximate the real one very well especially for the case of large unequally spaced arrays.

REFERENCES

- [1] A. Trucco, M. Palmese, and S. Repetto, "Devising an affordable sonar system for underwater 3-D vision," *IEEE Trans. Instrum. Meas.*, vol. 57, no. 10, pp. 2348–2354, Oct. 2008.
- [2] X. Hu, N. Tong, J. Wang, S. Ding, and X. Zhao, "Matrix completion-based MIMO radar imaging with sparse planar array," *Signal Process.*, vol. 131, pp. 49–57, Feb. 2017.
- [3] O. M. Bucci, T. Isernia, S. Perna, and D. Pinchera, "Isophoric sparse arrays ensuring global coverage in satellite communications," *IEEE Trans. Antennas Propag.*, vol. 62, no. 4, pp. 1607–1618, Apr. 2014.
- [4] B. Kumar and G. Branner, "Generalized analytical technique for the synthesis of unequally spaced arrays with linear, planar, cylindrical or spherical geometry," *IEEE Trans. Antennas Propag.*, vol. 53, no. 2, pp. 621–634, Feb. 2005.
- [5] O. M. Bucci and S. Perna, "A deterministic two dimensional density taper approach for fast design of uniform amplitude pencil beams arrays," *IEEE Trans. Antennas Propag.*, vol. 59, no. 8, pp. 2852–2861, Aug. 2011.
- [6] A. El-makadema, L. Rashid, and A. K. Brown, "Geometry design optimization of large-scale broadband antenna array systems," *IEEE Trans. Antennas Propag.*, vol. 62, no. 4, pp. 1673–1680, Apr. 2014.
- [7] P. You, Y. Liu, S.-L. Chen, K. Da Xu, W. Li, and Q. H. Liu, "Synthesis of unequally spaced linear antenna arrays with minimum element spacing constraint by alternating convex optimization," *IEEE Antennas Wireless Propag. Lett.*, vol. 16, pp. 3126–3130, 2017.
- [8] B. Fuchs, "Synthesis of sparse arrays with focused or shaped beam-pattern via sequential convex optimizations," *IEEE Trans. Antennas Propag.*, vol. 60, no. 7, pp. 3499–3503, Jul. 2012.
- [9] M. D'Urso, G. Prisco, and R. M. Tumolo, "Maximally sparse, steerable, and nonsuperdirective array antennas via convex optimizations," *IEEE Trans. Antennas Propag.*, vol. 64, no. 9, pp. 3840–3849, Sep. 2016.
- [10] Y. Liu, Z. Nie, and Q. H. Liu, "Reducing the number of elements in a linear antenna array by the matrix pencil method," *IEEE Trans. Antennas Propag.*, vol. 56, no. 9, pp. 2955–2962, Sep. 2008.
- [11] Y. Liu, Q. Huo Liu, and Z. Nie, "Reducing the number of elements in the synthesis of shaped-beam patterns by the forward-backward matrix pencil method," *IEEE Trans. Antennas Propag.*, vol. 58, no. 2, pp. 604–608, Feb. 2010.
- [12] H. Shen and B. Wang, "Two-dimensional unitary matrix pencil method for synthesizing sparse planar arrays," *Digit. Signal Process.*, vol. 73, pp. 40–46, Feb. 2018.
- [13] F. Viani, G. Oliveri, and A. Massa, "Compressive sensing pattern matching techniques for synthesizing planar sparse arrays," *IEEE Trans. Antennas Propag.*, vol. 61, no. 9, pp. 4577–4587, Sep. 2013.
- [14] W. Zhang, L. Li, and F. Li, "Reducing the number of elements in linear and planar antenna arrays with sparseness constrained optimization," *IEEE Trans. Antennas Propag.*, vol. 59, no. 8, pp. 3106–3111, Aug. 2011.
- [15] F. Yan, F. Yang, T. Dong, and P. Yang, "Synthesis of planar sparse arrays by perturbed compressive sampling framework," *IET Microw. Antennas Propag.*, vol. 10, no. 11, pp. 1146–1153, Aug. 2016.
- [16] T. N. Kaifas, D. G. Babas, G. S. Miaris, K. Siakavara, E. E. Vafadis, and J. N. Sahalos, "Aperiodic array layout optimization by the constraint relaxation approach," *IEEE Trans. Antennas Propag.*, vol. 60, no. 1, pp. 148–163, Jan. 2012.
- [17] P. Yuanding Zhou and M. Ingram, "Pattern synthesis for arbitrary arrays using an adaptive array method," *IEEE Trans. Antennas Propag.*, vol. 47, no. 5, pp. 862–869, May 1999.
- [18] D. Pinchera, M. D. Migliore, and G. Panariello, "Synthesis of large sparse arrays using idea (inflating-deflating exploration algorithm)," *IEEE Trans. Antennas Propag.*, vol. 66, no. 9, pp. 4658–4668, Sep. 2018.
- [19] A. Trucco, E. Omodei, and P. Repetto, "Synthesis of sparse planar arrays," *Electron. Lett.*, vol. 33, no. 22, pp. 1835–1843, 1997.
- [20] W. Keizer, "Large planar array thinning using iterative FFT techniques," *IEEE Trans. Antennas Propag.*, vol. 57, no. 10, pp. 3359–3362, Oct. 2009.
- [21] G. Oliveri, L. Manica, and A. Massa, "ADS-based guidelines for thinned planar arrays," *IEEE Trans. Antennas Propag.*, vol. 58, no. 6, pp. 1935–1948, Jun. 2010.
- [22] R. L. Haupt, "Optimized element spacing for low sidelobe concentric ring arrays," *IEEE Trans. Antennas Propag.*, vol. 56, no. 1, pp. 266–268, Jan. 2008.
- [23] R. Bhattacharya, T. K. Bhattacharyya, and R. Garg, "Position mutated hierarchical particle swarm optimization and its application in synthesis of unequally spaced antenna arrays," *IEEE Trans. Antennas Propag.*, vol. 60, no. 7, pp. 3174–3181, Jul. 2012.
- [24] S. Karimkashi and A. Kishk, "Invasive weed optimization and its features in electromagnetics," *IEEE Trans. Antennas Propag.*, vol. 58, no. 4, pp. 1269–1278, Apr. 2010.
- [25] A. Darvish and A. Ebrahimzadeh, "Improved fruit-fly optimization algorithm and its applications in antenna arrays synthesis," *IEEE Trans. Antennas Propag.*, vol. 66, no. 4, pp. 1756–1766, Apr. 2018.
- [26] C. Zhang, X. Fu, L. P. Lighthart, S. Peng, and M. Xie, "Synthesis of broadside linear aperiodic arrays with sidelobe suppression and null steering using whale optimization algorithm," *IEEE Antennas Wireless Propag. Lett.*, vol. 17, no. 2, pp. 347–350, Feb. 2018.
- [27] K. Chen, X. Yun, Z. He, and C. Han, "Synthesis of sparse planar arrays using modified real genetic algorithm," *IEEE Trans. Antennas Propag.*, vol. 55, no. 5, pp. 1067–1073, Apr. 2007.
- [28] H. Liu, H. Zhao, W. Li, and B. Liu, "Synthesis of sparse planar arrays using matrix mapping and differential evolution," *IEEE Antennas Wireless Propag. Lett.*, vol. 15, pp. 1905–1908, 2016.
- [29] D. Dai, M. Yao, H. Ma, W. Jin, and F. Zhang, "An asymmetric mapping method for the synthesis of sparse planar arrays," *IEEE Antennas Wireless Propag. Lett.*, vol. 17, no. 1, pp. 70–73, Jan. 2018.
- [30] M. D. Gregory, F. A. Namin, and D. H. Werner, "Exploiting rotational symmetry for the design of ultra-wideband planar phased array layouts," *IEEE Trans. Antennas Propag.*, vol. 61, no. 1, pp. 176–184, Jan. 2013.
- [31] T. G. Spence and D. H. Werner, "Design of broadband planar arrays based on the optimization of aperiodic tilings," *IEEE Trans. Antennas Propag.*, vol. 56, no. 1, pp. 76–86, Jan. 2008.

- [32] Y. Wang, H. Liu, H. Long, Z. Zhang, and S. Yang, "Differential evolution with a new encoding mechanism for optimizing wind farm layout," *IEEE Trans. Ind. Informat.*, vol. 14, no. 3, pp. 1040–1054, Mar. 2018.
- [33] R. Storn and K. Price, "Differential evolution—A simple and efficient heuristic for global optimization over continuous spaces," *J. Global Optim.*, vol. 11, no. 4, pp. 341–359, 1997.
- [34] D. Kurup, M. Hmida, and A. Rydberg, "Synthesis of uniform amplitude unequally spaced antenna arrays using the differential evolution algorithm," *IEEE Trans. Antennas Propag.*, vol. 51, no. 9, pp. 2210–2217, Sep. 2003.
- [35] M. Li, Y. Liu, and Y. J. Guo, "Shaped power pattern synthesis of a linear dipole array by element rotation and phase optimization using dynamic differential evolution," *IEEE Antennas Wireless Propag. Lett.*, vol. 17, no. 4, pp. 697–701, Apr. 2018.
- [36] Y. Chen, S. Yang, and Z. Nie, "The application of a modified differential evolution strategy to some array pattern synthesis problems," *IEEE Trans. Antennas Propag.*, vol. 56, no. 7, pp. 1919–1927, Jul. 2008.
- [37] W. Feller, *An Introduction to Probability Theory and its Applications*, 3rd ed. New York, NY, USA: Wiley, 1968.
- [38] H. G. Schuster, *Deterministic Chaos: Introduction*. Weinheim, Germany: Physik-Verlag, 1988.
- [39] X. Yao, Y. Liu, and G. Lin, "Evolutionary programming made faster," *IEEE Trans. Evol. Comput.*, vol. 3, no. 2, pp. 82–102, Jul. 1999.
- [40] Y. Liu, S.-L. Chen, L. Zhang, and Q. H. Liu, "Determining the first-null mainlobe region of an arbitrary pattern for 2-D numerical pattern synthesis algorithm," *IEEE Trans. Antennas Propag.*, vol. 64, no. 3, pp. 1130–1136, Mar. 2016.



Foxiang Liu was born in Ganzhou, China, in 1991. He received the M.S. degree in computational mathematics from Nanjing Normal University, Nanjing, China, in 2017. He is currently pursuing the Ph.D. degree with the Institute of Electromagnetics and Acoustics, Xiamen University, Xiamen, China.

His current research interests include antenna array designs, computational intelligence, and convex optimization. He has authored and coauthored several peer-reviewed journal articles and conference papers.



Yanhui Liu (Senior Member, IEEE) received the B.S. and Ph.D. degrees in electrical engineering from the University of Electronic Science and Technology of China (UESTC), Chengdu, China, in 2004 and 2009, respectively.

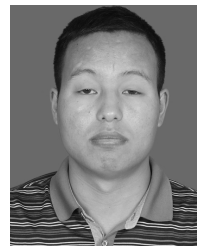
From September 2007 to June 2009, he was a Visiting Scholar with the Department of Electrical Engineering, Duke University, Durham, NC, USA. In July 2011, he joined the Department of Electronic Science, Xiamen University, Xiamen, China, where he was lately promoted as a Full Professor. From September to December 2017, he was a Visiting Professor with the State Key Laboratory of Millimeter Waves, City University of Hong Kong, Hong Kong. Since December 2017, he has been with the Global Big Data Technologies Centre, University of Technology Sydney (UTS), Ultimo, NSW, Australia, as a Visiting Professor/Research Principal. Since January 2020, he has been a Professor with UESTC, where he is supported by the 100 Talents Plan of UESTC. He has authored and coauthored over 140 peer-reviewed journal articles and conference papers. He holds 13 granted Chinese invention patents. His research interests include antenna array design, reconfigurable antennas, and electromagnetic signal processing.

Dr. Liu received the UESTC Outstanding Graduate Award in 2004 and the Excellent Doctoral Dissertation Award of Sichuan Province of China in 2011. He is serving as a reviewer for a dozen of SCI-indexed journals. Since 2018, he has served as an Associate Editor for IEEE ACCESS. He has served many times as a TPC Member or a Reviewer for the IEEE APS, the Progress in Electromagnetics Research Symposium (PIERS), the Asia-Pacific Conference on Antennas and Propagation (APCAP), and the National Conference on Antenna (NCANT), and a Session Chair for NCANT2015, PIERS2016/2019, ACES2017-China, NCANT2017, APCAP2017, and ICCEM2018/2019.



Feng Han (Member, IEEE) received the B.S. degree in electronic science from Beijing Normal University, Beijing, China, in 2003, the M.S. degree in geophysics from Peking University, Beijing, in 2006, and the Ph.D. degree in electrical engineering from Duke University, Durham, NC, USA, in 2011.

He is currently an Assistant Professor with the Institute of Electromagnetics and Acoustics, Xiamen University, Xiamen, China. His research interests include ionosphere remote sensing by radio atmospherics, electromagnetic full-wave inversion by integral equations, reverse time migration image, and the design of an electromagnetic detection systems.



Yong-Ling Ban was born in Henan, China. He received the B.S. degree in mathematics from Shandong University, Jinan, China, in 2000, the M.S. degree in electromagnetics from Peking University, Beijing, China, in 2003, and the Ph.D. degree in microwave engineering from the University of Electronic Science and Technology of China (UESTC), Chengdu, China, in 2006.

In July 2006, he joined the Xi'an Mechanical and Electrical Information Institute, Xi'an, China, as a Microwave Engineer. He then joined Huawei Technologies Co., Ltd., Shenzhen, China, where he designed and implemented various terminal antennas for 15 data card and mobile phone products customized from leading telecommunication industries like Vodafone. From September 2010 to July 2016, he was an Associate Professor with UESTC, where he is currently a Professor. From May 2014 to April 2015, he visited the Queen Mary University of London, London, U.K., as a Scholar Visitor. His research interests include wideband small antennas for 4G/5G handset devices, MIMO antenna, and millimeter wave antenna array. He is the author of over 110 referred journal articles and conference papers on these topics. He holds 30 granted and pending Chinese and overseas patents.



Y. Jay Guo (Fellow, IEEE) received the bachelor's and master's degrees from Xidian University, Xi'an, China, in 1982 and 1984, respectively, and the Ph.D. degree from Xian Jiaotong University, Xi'an, in 1987.

His research interest includes antennas, mm-wave and THz communications and sensing systems, and big data technologies. He has published over 470 research articles, including 250 journal articles and holds 26 patents in antennas and wireless systems.

Dr. Guo was a member of the College of Experts of Australian Research Council (ARC) from 2016 to 2018. He is a fellow of the Australian Academy of Engineering and Technology and the Institution of Engineering and Technology (IET). He has won a number of most prestigious Australian Engineering Excellence Awards in 2007 and 2012 and the CSIRO Chairmans Medal in 2007 and 2012. He was named one of the most influential engineers in Australia in 2014 and 2015. He is also a Distinguished Professor and the Director of the Global Big Data Technologies Centre (GBDTc), University of Technology Sydney (UTS), Ultimo, NSW, Australia. Prior to this appointment in 2014, he served as a Director for CSIRO for over nine years. Before joining CSIRO, he held various senior technology leadership positions in Fujitsu, Siemens, and NEC in the U.K. He has chaired numerous international conferences and served as guest editors for a number of IEEE publications. He is the Chair of the International Steering Committee and the International Symposium on Antennas and Propagation (ISAP). He was the International Advisory Committee Chair of the IEEE VTC2017, the General Chair of ISAP2022, ISAP2015, iWAT2014, and WPMC'2014, and the TPC Chair of 2010 IEEE WCNC and 2012 and 2007 IEEE ISCIT. He served as a Guest Editor for special issues on *Antennas for Satellite Communications* and *Antennas and Propagation Aspects of 60–90 GHz Wireless Communications* from the IEEE TRANSACTIONS ON ANTENNAS AND PROPAGATION, special issue on *Communications Challenges and Dynamics for Unmanned Autonomous Vehicles* from the IEEE JOURNAL ON SELECTED AREAS IN COMMUNICATIONS (JSAC), and special issue on *5G for Mission Critical Machine Communications*, and *IEEE Network Magazine*.